A Non-Empirical Intermolecular Potential for Oxalic Acid Crystal Structures

Irene Nobeli[†] and Sarah L. Price*

Centre for Theoretical and Computational Chemistry, University College London, 20 Gordon Street, London WC1H 0AJ, U.K.

Received: March 26, 1999; In Final Form: June 10, 1999

A model intermolecular potential for oxalic acid is derived from the properties of the isolated molecule. Various methods of obtaining an isotropic atom−atom repulsion potential from the overlap of the monomer charge distributions are investigated. These model repulsion potentials are combined with an electrostatic model based on a distributed multipole analysis of the monomer wave function and a Slater−Kirkwood dispersion model using atomic polarizabilities. The resulting model potentials are tested for their ability to reproduce the two crystal forms of oxalic acid. The best models do reasonably well, within the limitations of static lattice energy minimization of rigid molecules. Since current transferable empirical model potentials used for modeling carboxylic acid crystal structures have problems in accounting for the oxalic acid polymorphs, this success shows the benefits of deriving specific model atom−atom potentials for organic molecules without relying on transferability assumptions.

1. Introduction

The intermolecular forces between organic molecules are generally represented using an empirical repulsion−dispersion model in which the parameters for the different types of atoms are assumed to be transferable between all molecules of that class (e.g., carboxylic acids). In contrast, the electrostatic model is often derived specifically for the molecule and reflects the effects of hybridization and bonding environment on the valence electron distribution. (These effects are more accurately represented by distributed multipole representations of the charge distribution, with the anisotropic multipole moments representing features such as lone pairs and π electrons, than atomic point charge models[1,2]). Thus the variations in the atomic charge distributions between molecules with different bonding environments are completely ignored in the derivation of the repulsion−dispersion potential.

This assumption has been found adequate for deriving intermolecular potentials for modeling the crystal structures of large numbers of organic molecules. Many sets of atom−atom repulsion and dispersion potentials have been empirically fitted to the crystal structures of several related molecules[3] such as the azahydrocarbons[4] and oxohydrocarbons[5] in conjunction with a specific electrostatic model, or amides[6] and carboxylic acids[7] with a transferable electrostatic model, and even a large range of organic compounds with no explicit electrostatic model.[8,9] A transferable set of $C/H_C/O/N/H_N$ repulsion−dispersion parameters, in conjunction with a distributed multipole model for the electrostatic forces,[10] can reproduce a wide range of polar organic crystal structures involving heterocycles, nitro, amide, amine groups within acceptable accuracy for static lattice energy minimization. However, in most of these studies, there are a few crystal structures which are not reproduced satisfactorily, for various reasons. There may be a feature of the molecular packing which is very sensitive to the model potential, so that the crystal structure distorts considerably for little change in the lattice energy, thus requiring a highly accurate potential. Sometimes, the "rogue" crystal structure is sensitive to aspects of the potential that are not sampled by the crystal structures of other members of the family, for example, *s*-tetrazine ($C_2H_2N_4$) samples the N···N repulsive wall unlike other azabenzenes,[11] so there is not enough data to determine this aspect of the potential by empirical fitting. It may be that the transferability assumption is no longer adequate because the charge distribution within a functional group differs significantly from that in other molecules in the family. Often the crystal structures which are poorly modeled by the transferable potentials are those of the smaller, more symmetric molecules in a series.

Oxalic acid is one such example, as many transferable potential schemes are unable to reproduce both of the known polymorphs satisfactorily. Simple exp-6 model potentials,[9] derived considering the crystal structures of 91 monocarboxylic acids and 82 bicarboxylic acids, were unusually poor for the structures of oxalic acid, which was attributed to inadequacies in the C···O potential. Another commonly used set of empirical potentials which were fitted to reproduce a range of carboxylic acids, the Lennard−Jones plus point charge models of Hagler and Lifson,[7] have outstandingly large deviations for the structures of oxalic acid.[12] The very heavily parameterized empirical potentials for small carboxylic acids of Derissen and Smit[13] do appear to reproduce both structures satisfactorily, but when these authors derived alternative ab initio based model potentials,[14] the optimization of the β-oxalic acid structure was notably difficult and the calculated energies were generally in error by about 30%. Thus, the packings of the two hydrogen-bonded networks of oxalic acid, though having features in common with other carboxylic acids,[15] appear to be quite a sensitive test of the model for the intermolecular forces. The problems with reproducing these structures are not due to the inadequacy of using an atomic point charge[7,13,14] or no explicit[9] electrostatic model. A potential scheme, based on a distributed multipole electrostatic model, and polar hydrogen parameters specifically optimized to reproduce the hydrogen bond lengths

* E-mail: s.l.price@ucl.ac.uk. Fax: 44 (0)171 380 7463.
[†] Current address: Department of Biochemistry and Molecular Biology, University College London, Darwin Building, Gower Street, London, WC1, U.K.

10.1021/jp9910643 CCC: $18.00
Published on Web 07/23/1999

in carboxylic acids,[16] can reproduce the crystal structures of formic, acetic, benzoic, both polymorphs of tetrolic and fumaric, and α-oxalic acid satisfactorily, but not β-oxalic acid. The two polymorphs of oxalic acid sample more regions of the potential surface for the interaction of two carboxylic groups than the other carboxylic acids, and the lack of any hydrocarbon group from which to draw electron density makes the CO_2H groups of oxalic acid atypical, so it is plausible that oxalic acid crystals are poorly modeled by transferable model potentials.

Thus we need a method of deriving model intermolecular potentials specific to the organic molecule for such cases where transferable potentials are inadequate. Fitting to ab initio potential energy surfaces is widely used to derive intermolecular potentials for small polyatomics, but this is impracticable for organic molecules as it requires the calculation of a very high quality correlated wave function[17] for the dimer at thousands of relative orientations. Thus, the intermolecular potential has to be built up from its component contributions,[18] with each contribution being parameterized separately using the properties of the isolated molecule. There have been several variants on this approach implemented,[19,20] mainly for small polyatomics. Although the electrostatic component can be readily modeled for quite large organic molecules,[2] the schemes for modeling the repulsion, dispersion, and other contributions need to be tested and developed for organic molecules. In this paper, we develop a systematic approach based on using the overlap model for the repulsion[21] and apply it to give a model intermolecular potential for oxalic acid, which is tested for its ability to reproduce the crystal structures.

The overlap model assumes that the exchange−repulsion between two closed shell molecules (A and B) is proportional to the overlap of the isolated molecule charge densities (ρ_A and ρ_B) at the required relative orientation of the molecules, found by integrating over the spatial coordinates **r**

$$U_{\text{rep}} = KS^{\rho} = K \int \rho_A(\mathbf{r})\rho_B(\mathbf{r})d\mathbf{r} \tag{1}$$

Since ρ_B is the charge density of the second molecule B positioned at a separation R and orientation Ω relative to molecule A, this gives a model for the orientation dependence of the intermolecular potential

$$U_{\text{rep}}(R,\Omega) = KS^{\rho}(R,\Omega) \tag{2}$$

This assumption has been tested explicitly and is found to give a reasonable prediction for pairs of rare gas atoms,[22] rare gas atoms with halide ions,[23] $(F_2)_2$, $(N_2)_2$, $(Cl_2)_2$,[21] and more recently the N···H−O hydrogen bonding regions of the pyridine/methanol and methylcyanide/methanol potentials.[24] Since the overlap is relatively cheap to calculate, it can be obtained at sufficient points to sample the repulsive wall and used to parameterize a model potential form by fitting. This has provided model potentials, which successfully account for spectroscopic properties of the hydrazine dimer[25,26] and methanol clusters,[27] have been used to predict the properties of $Li^+\cdots H_2O$[28] and successfully model the hydration of Na^+ from $Na^+\cdots H_2O$ and $(H_2O)_2$ potentials.[29] Applied in this way, the overlap model competes with alternative assumptions about the intermolecular repulsion which are used to make the computation of sufficient points of the repulsion potential energy surface practicable. Examples of these are fitting to the overlap of the wave functions (as used in NEMO[30]), or the fitting to the ab initio interactions of the molecule with a test particle such as He, and subsequent assumption of combining rules.[31] However, all of these methods have the partitioning of the total model repulsion into atom−atom contributions determined by a fitting procedure, which can be poorly conditioned for regions when more than one atom's repulsive wall is being sampled, for example, in hydrogen bonds. One major advantage of the overlap model is that it can provide a partitioning into atom−atom repulsion contributions, by first partitioning the molecular charge distribution into extended atomic charge distributions,[32] each described by a set of Gaussian functions. This partitioning allows each atom−atom overlap S_{ik} (for atom i in molecule A and k in molecule B) to be calculated separately. An analytical expression for the orientation dependence of each atom−atom overlap at a given atom−atom separation can also be obtained, using the properties of the Gaussian functions,[21] giving an anisotropic atom−atom model repulsion potential

$$U_{\text{rep}} = K \sum_{i\in A,k\in B} S_{ik}^{\rho}(R_{ik}, \Omega_{ik}) \tag{3}$$

The analytical expressions for the atom−atom overlap at a range of separations can be analyzed (as described in the methods section) to give an isotropic atom−atom exponential model for the atom−atom overlap

$$S_{ik}^{\rho}(R_{ik}, \Omega_{ik}) \approx s_{\iota\kappa} \exp(-\alpha_{\iota\kappa}R_{ik}) \tag{4}$$

where s and α are constant parameters for a given atomic types ι and κ of atoms i and k. Thus, this approach provides an atom−atom representation of the overlap, which by assumption of a scaling factor K, gives an isotropic atom−atom model repulsion in the usual form

$$U_{\text{rep}} \approx \sum A_{\iota\kappa} \exp(-B_{\iota\kappa}R_{ik}) \approx K \sum s_{\iota\kappa} \exp(-\alpha_{\iota\kappa}R_{ik}) \tag{5}$$

with the pre-exponential repulsion coefficient $A_{\iota\kappa} = Ks_{\iota\kappa}$ and the same exponential decay. Thus, we obtain a model of the exchange repulsion between two organic molecules, in an isotropic atom−atom form, from the ab initio charge densities of the isolated molecules. There is only one parameter, K, to be determined by fitting to either experimental or ab initio data. This paper develops this novel approach for determining the repulsion between organic molecules and tests it by considering the crystal structures of the oxalic acid polymorphs.

We assume a model potential that explicitly models only the electrostatic, repulsion, and dispersion forces. The electrostatic forces are represented quite accurately by a distributed multipole model[33] and are expected to dominate the orientation dependence of the potential. The repulsion potential will particularly affect the van der Waals separations and is the main focus of this investigation. Since it is not yet feasible to derive an accurate atom−atom model for the dispersion interactions between molecules the size of oxalic acid from their charge distribution, we have used a simple Slater−Kirkwood dispersion model[34] using atomic polarizabilities to estimate an isotropic atom−atom C_6 coefficient. Thus the model potential neglects the atom−atom anisotropy in the repulsion and dispersion, the higher order terms in the dispersion, the polarization, charge transfer, and penetration energy, and the modification of the other long-range terms due to the overlap of the charge distributions. This gives a potential that is derived mainly from the charge density of the molecule, and without any reference to experimental data on oxalic acid or other carboxylic acids, or to calculations of the total interaction energy.

2. Method

Oxalic acid has two known polymorphs with different hydrogen bonding geometries. α-Oxalic acid is based on highly

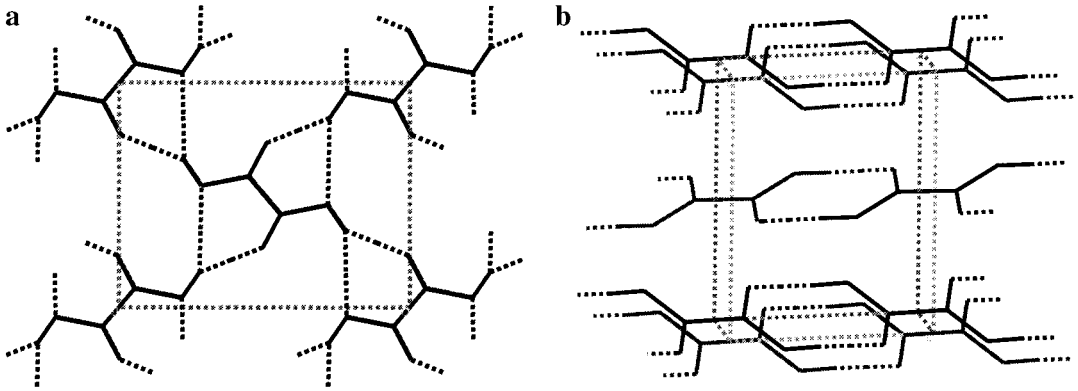

Figure 1. The hydrogen bonding motifs and crystal structures of the two polymorphs of oxalic acid. (a) The crinkled sheet structure of α-oxalic acid projected onto the *bc* plane (*b*-axis horizontal, *c*-axis vertical), with $O_2-H\cdots O_1$ hydrogen bonds ($O_2\cdot\cdot O_1$ 2.702 Å) forming a chain. There are also elongated $O_2-H\cdots O_2$ hydrogen bonds ($O_2\cdot\cdot O_2$ 3.110 Å). The related sheet at *a*/2 is not shown for clarity. (b) The chains of carboxylic acid dimers in the $R^2_2(8)$ graph set[59] motif in *β*-oxalic acid, as viewed with the *a*-axis horizontal and the *b*-axis vertical. The $O_1\cdot\cdot O_2$ hydrogen bonded distance is 2.674 Å.

corrugated hydrogen-bonded sheets, with a conventional hydrogen bond from $-O_2-H$ forming to $=O_1$ and an elongated hydrogen bond to $-O_2-$, both in the direction of the exterior of the carboxyl group, as shown in Figure 1a. The sheets stack along the *a* direction in space group *Pcab* with $a = 6.548$ Å, $b = 7.844$ Å, and $c = 6.086$ Å in the room-temperature X-ray structure determination.[35] The *β* polymorph is based on the carboxylic acid dimer motif (Figure 1b), forming infinite ribbons along the *a*-axis, so that the molecular and hydrogen bond lengths determine $a = 5.330$ Å. The ribbons are stacked in a herringbone fashion, with $b = 6.015$ Å, $c = 5.436$ Å, and the angle $\beta = 115.83°$ defines the relative offset of the chains in the $P2_1/c$, $Z' = 0.5$ room-temperature crystal structure.[35] Thus the two polymorphs sample different aspects of the intermolecular potential, as reflected by their dramatically different Hirshfeld surfaces,[36] the molecular surfaces defined by stockholder partitioning of the electron density in the crystals.

In the crystal structure modeling, the geometries for the oxalic acid molecule were taken directly from the crystal structures using the Cambridge Structural Database[37] entries OXALAC03 (α form) and OXALAC04 (*β* form), and thus reflect the small differences in the carboxylic group geometries and nonplanarity of the molecules. The O−H distance was elongated to 1.02 Å, a neutron diffraction average observed for carboxylic acids,[38] to allow for the systematic error in the location of hydrogen atoms by X-ray diffraction. These molecular geometries were assumed rigid in the crystal structure modeling, and define the position of the interaction sites in the various model potentials of the form

$$U = \sum_{i\in A,k\in B} A_{\iota\kappa} \exp(-\alpha_{\iota\kappa} R_{ik}) - \frac{C_{\iota\kappa}}{R_{ik}^6} + U_{\text{electrostatic}}\,(DMA, R_{ik}^n, n \le 5) \quad (6)$$

The atomic types required for oxalic acid (assuming gas-phase symmetry) are ι, κ = C, O_1, O_2, or H, where the two oxygens are distinguished by their coordination number, i.e., $C=O_1$ and $C-O_2-H$. For each model potential, the lattice energy was minimized, starting from each of the two observed structures, using the program DMAREL.[39] This finds a minimum in the lattice energy by minimizing the strain matrix for the unit cell and optimizing the translation and rotation of each molecule in the unit cell.

2.1 Derivation of the Repulsion Parameters. The repulsion potential was based on the geometry of the oxalic acid monomer optimized at the MP2 level with a 6-31G** basis set, using the program suite CADPAC.[40] The charge distribution at the MP2 level was calculated for four different basis sets to test the sensitivity of the overlap model to the description of the charge density. The basis sets considered were a standard split valence polarized basis 6-31G**,[41] a 6-311G** basis set[42] which has an additional set of valence orbitals, a correlation consistent polarized valence double-ζ basis set (cc-pVDZ)[43] where the polarization functions are optimized by considering the correlation energy, and the latter basis set augmented with an additional diffuse function for each angular momentum type (aug-cc-pVDZ).[43] Each charge density of oxalic acid was re-expressed in terms of atom-centered Gaussian multipoles using the program GMUL3.[32] The standard GMUL simplification of exponents procedure was used to reduce the number of Gaussians used to represent the inner portions of the atomic charge densities.

An analytical expression for the atom−atom overlap of charge densities for a fixed atom−atom separation R_{ik} in the oxalic acid dimer was obtained using GMUL 3s [44] in the form

$$S_{ik}^{\rho}(\Omega_{ik}) = \sum C_{l_1 l_{2j}}^{k_1 k_2} S_{l_1 l_{2j}}^{k_1 k_2}(\Omega_{ik}) \quad (7)$$

where the coefficients $C_{l_{11}l_{2j}}^{k_1k_2}$ depend on the atom−atom separation, and $S_{l_{11}l_{2j}}^{k_1k_2}$ are the nonnormalized set of orthogonal orientation dependent functions developed by Stone,[45] with $S_{000}^{00} = 1$. The overlap was calculated between all atom−atom pairs at five interatomic separations, R_{ik}, within 0.25 Å of the sum of the van der Waals radii for the atoms (1.52 Å for O, 1.70 Å for C, and 1.09 Å for H). For H···O and O···O contacts seven interatomic separations were calculated, to cover the short hydrogen bonded contacts observed in the crystals. For the H···O contacts the separations were centered around 3.7 Bohr (∼1.95 Å), taking this as a typical hydrogen bond separation. Ignoring the anisotropy of the atom−atom overlap, the isotropic *S*-function coefficients C_{000}^{00} were used to derive a model for the atom−atom overlap $s_{\iota\kappa}{}^{\text{anal}}\exp(-\alpha_{\iota\kappa}R_{\text{ik}})$ by a linear regression of the negative logarithm of C_{000}^{00} over the interatomic separation R_{ik} using the EXCEL[46] program. This provided an isotropic atom−atom model for the overlap of the charge distributions

$$S^{\rho,\text{model}} = \sum_{i\in Ak\in B} s_{\iota\kappa} \exp(-\alpha_{\iota\kappa} R_{ik}) \quad (8)$$

for each ab initio charge density considered. (Any charge density where the atom−atom overlaps did not show the expected

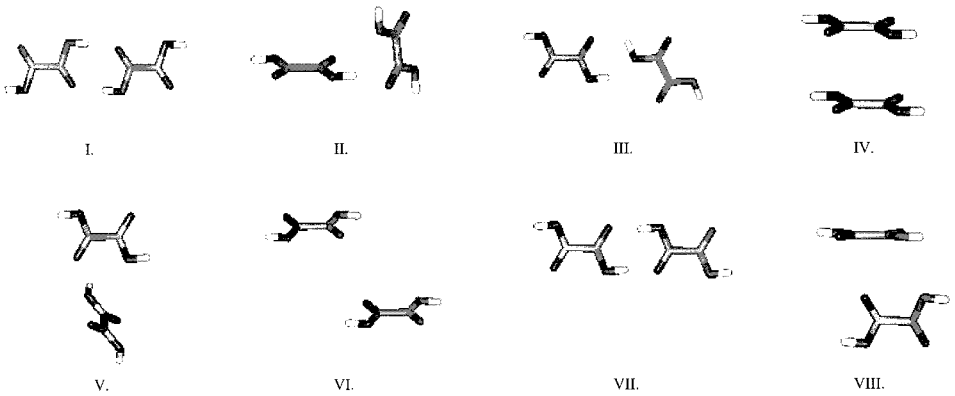

Figure 2. The eight geometries used in IMPT calculations to estimate the proportionality constant between overlap and repulsion. I, II, and II are minima in the MP2/6-31G** DMA + exp-6 (FIT[10]) potential surface of the oxalic acid dimer, as found using the program ORIENT.[60] IV is a local minimum in the corresponding MP2/aug-cc-pVDZ surface. V and VI are taken directly from the crystal structure OXALAC03 (α form), and VII and VIII from OXALAC04 (β form). Geometries I and VII differ in the hydrogen bond length, as do geometries II and V.

exponential decay, and so gave a poor fit with a correlation coefficient less than about 0.99, was immediately suspect.)

An estimate of the proportionality constant between the overlap and the exchange repulsion was made by fitting K in

$$U_{\text{rep}} = KS^{\rho,\text{model}} = K \sum_{i\in A, j\in B} s_{\iota\kappa} \exp(-\alpha_{\iota\kappa} R_{ik}) \qquad (9)$$

to E_{er}, the exchange-repulsion energy evaluated by intermolecular perturbation theory (IMPT),[47−49] for the eight geometries of the oxalic acid dimer shown in Figure 2. This gives the exchange-repulsion energy at first order in perturbation theory corresponding to the SCF 6-31G** charge densities of the isolated molecules. The proportionality constant K was fitted, using eight geometries, spanning both hydrogen bonded and stacked configurations, with the quality of the fit testing the overlap assumption. This fitting gave a proportionality constant, K, for each of the four different basis sets. For each basis set, the set of $Ks_{\iota\kappa}$ and $\alpha_{\iota\kappa}$ parameters was used as the repulsion parameters in the crystal structure minimization program DMAREL.

Observations made in a study of the use of the anisotropic expansion of the overlap model to fit the IMPT exchange-repulsion surface of the hydrogen bond from methanol to pyridine and methylcyanide suggested two variations in the above method which we investigated, as described below, in addition to the basis set dependence.

2.1.1 Fitting the Pre-exponential Parameters to Atom−Atom Overlaps. Deriving both the $s_{\iota\kappa}$ and $\alpha_{\iota\kappa}$ parameters from the isotropic overlap coefficient leaves no possibility for the neglected anisotropic terms to be absorbed into the model potential. Since the analytical expansion of the overlap of two atomic charge distributions given by GMUL treats the region around each atom in the direction of the intramolecular bonds on an equal footing to the intermolecular contact region, the isotropic coefficient C_{000}^{00} is unlikely to be the optimum isotropic coefficient for the intermolecular repulsion. Thus, an alternative to the above method of obtaining the $s_{\iota\kappa}$ parameters is to fit them to a range of atom−atom overlaps for orientations in the intermolecular contact region. These total atom−atom overlaps can be calculated using the program GMUL as an alternative to their analytical expansion. By using the GMUL division of the overlap into atom−atom contributions and assuming that the exponents $\alpha_{\iota\kappa}$ for the model isotropic overlap were accurately obtained from the isotropic coefficient, only the pre-exponential factors $s_{\iota\kappa}$ needed fitting. Thus far fewer points were required than would be necessary for fitting the complete model potential to an overlap surface. We restricted the calculation of the atom−atom contributions to the total overlap integral to 17 geometries, eight of which resembled the geometries used for the IMPT calculations and the rest were all based on these eight with the two monomers simply brought closer or pushed further apart. This guaranteed a minimum of five atom−atom overlap values at distances within the limits of the distances used in the isotropic coefficient calculations for each atom−atom pair. (For some atomic pairs, all overlap values came from the same orientation of the two molecules, and so this did not test how effectively the new isotropic overlap model reproduced the anisotropy of the overlap in the intermolecular region.) This approach gives a set of fitted s_{ik}^{fit} values, which were used with the appropriate proportionality constant K, to give an alternative repulsion model.

2.1.2 Using Exponent Values Calculated from Large Basis Set Calculations. The linear regression analysis showed that there is considerable correlation between the pre-exponential factor $s_{\iota\kappa}$ and the exponent $\alpha_{\iota\kappa}$ when they are derived from the $C_{000}^{00}(R_{ik})$ data, with different basis sets giving very similar overlaps but considerable variation in both the $\alpha_{\iota\kappa}$ and $s_{\iota\kappa}$ values. Some of this variation can be attributed to the overlap not exactly following the expected exponential decay because a limited number of Gaussian primitives is unable to model the tail of the charge density very accurately. Hence, we also calculated an MP2 charge density for formic acid using an *8s6p3d* basis set,[40] a basis set that is too large for us to use on oxalic acid, let alone larger organic molecules. This was subject to a GMUL analysis and a set of $\alpha_{\iota\kappa}$ formic acid parameters derived by fitting C_{000}^{00} against R_{ik} for the formic acid dimer. The exponents $\alpha_{\iota\kappa}^{\text{formic}}$ were assumed to be transferable to oxalic acid, and the corresponding new set of $s_{\iota\kappa}$ oxalic acid parameters were derived by fitting to the atom−atom overlaps as in section 2.1.1.

Thus, we investigated three types of overlap model for the repulsion: the analytic model where both the $s_{\iota\kappa}^{\text{anal}}$ and $\alpha_{\iota\kappa}$ values are derived from the C_{000}^{00} data, the fitted pre-exponential model where the $s_{\iota\kappa}^{\text{fit}}$ value was fitted to a small set of overlaps in the intermolecular repulsion region, and the transferable exponent model where the $\alpha_{\iota\kappa}^{\text{formic}}$ values were transferred from an analytic model for formic acid, calculated using a large basis set with accurate exponential decay of the wave function, and the pre-exponential $s_{\iota\kappa}$ parameters were refitted to the oxalic acid overlap values. Each type of repulsion model was investigated for various basis sets, in conjunction with the electrostatic model derived for the corresponding basis set and a fixed dispersion model.

2.2 Derivation of the Dispersion Model. The Slater−Kirkwood approximation was used.[34] This relates the dispersion contribution from two atoms in different molecules to their polarizabilities and the number of their valence electrons

$$C_{\iota\kappa} = \frac{3}{2}\frac{\alpha_\iota \alpha_\kappa}{(\alpha_\iota/N_\iota^{\text{eff}})^{1/2} + (\alpha_\kappa/N_\kappa^{\text{eff}})^{1/2}} \qquad (10)$$

where $C_{\iota\kappa}$ is the dispersion coefficient for the interaction of atoms of types ι and κ of polarizabilities α_ι and α_κ, and with N_ι^{eff} and N_κ^{eff} number of "effective" valence electrons, correspondingly. This number was taken here to equal the number of valence electrons for each atom, although it has been argued that this may be an underestimate.[50] Atomic polarizabilities were taken from Ketelaar [51] using 0.93 Å^3 for C, 0.42 Å^3 for H, 0.59 Å^3 for hydroxyl O_2, and 0.84 Å^3 for carbonyl O_1. Thus, the dispersion potential does distinguish between the two types of oxygen in oxalic acid. Nevertheless, it is a crude first estimate of the long-range dispersion potential.

2.3 Derivation of the Electrostatic Model. The electrostatic model comprised the atomic multipoles obtained by a distributed multipole analysis[33] of the MP2 wave functions for the same basis set (6-31G**, 6-311G**, cc-pVDZ, or aug-cc-pVDZ) as the repulsion model, calculated using the experimental molecular geometries (with the H−O distances normalized) using CADPAC. The electrostatic contribution to the lattice energy was evaluated for all terms in the intermolecular atom−atom multipolar expansion up to R^{-5}, using Ewald summation for the charge−charge, charge−dipole and, dipole−dipole terms, and direct summation for all other terms, using a cutoff of 15 Å in the center of mass separation. The repulsion−dispersion contributions to the lattice energy were also evaluated by direct summation to 15 Å, based on an atom−atom cutoff.

3. Results

3.1 Derivation of the Repulsion Parameters. The isotropic coefficient of the overlap expansion C_{000}^{00} had the expected exponential variation with distance for all 10 different atom−atom interactions for most of the basis sets investigated, and thus could be used to extract the α slope parameters. The least-squares fit of

$$\ln C_{000}^{00}(R_{\iota\kappa}) = \ln s_{\iota\kappa} - \alpha_{\iota\kappa} R_{ik} \qquad (11)$$

had r^2 fits of 0.999 for all atom−atom pairs for the 6-31G**, 6-311G**, and cc-pVDZ basis sets (with the minor exception of H···H for the 6-311G** basis set). However, the aug-cc-pVDZ MP2 charge densities, where many of the overlaps involving the H and O atoms were poorly fitted with r^2 values down to 0.923 for $O_1\cdots O_1$, gave $\alpha_{\iota\kappa}$ values which were very different from those given by the other basis sets. In contrast, the large basis set calculations on the formic acid dimer gave r^2 values better than 0.9999 for all atom−atom types, and $\alpha_{\iota\kappa}$ values that were generally similar or slightly smaller than those derived from smaller basis sets for oxalic acid. Thus, although the method does allow for the slope parameters to be readily derived, the results are sensitive to how the basis set describes the radial dependence of the charge distribution, with the basis set which had been augmented with a number of diffuse Gaussian basis functions (aug-cc-pVDZ) being particularly unsuitable.

The comparison of the overlap values and the calculated exchange−repulsion energy at the eight geometries in Figure 2 also provides a check on the model. All four basis sets give a good correlation (Table 1) between the total intermolecular overlap, S^ρ, and the exchange−repulsion at these geometries, though it is poorer for the aug-cc-pVDZ basis set, confirming that the basic overlap assumption is reasonable. However, when the derived sets of $\alpha_{\iota\kappa}$ and $s_{\iota\kappa}^{\text{anal}}$ parameters (Table 2) were used to calculate the total atom−atom overlap (eq 9), and these were compared with the eight IMPT exchange−repulsion energies, the fits were still reasonable ($r^2 \sim 0.98$) for all but the aug-cc-pVDZ basis set ($r^2 < 0.3$) which was clearly giving hopeless estimates of the repulsion (Table 1). Thus the division of the charge density into atomic contributions, and the assumption of an isotropic atom−atom repulsion model, are clearly the main reason why the aug-cc-pVDZ basis set, with its additional diffuse functions, is unsuitable for deriving overlap model repulsion parameters. The proportionality constants, K, between the overlap and the exchange−repulsion energy, vary somewhat with basis set and also change between the fits of the total overlap and the model isotropic atom−atom overlap for the same basis set. This is presumably absorbing some of the error in the isotropic atom−atom approximation, and so the latter K values were used to multiply the overlap pre-exponentials $s_{\iota\kappa}$ to give the repulsion pre-exponential parameters $A_{\iota\kappa}$ as in eqs 5 and 9.

TABLE 1: The Proportionality Factors K (in a.u.) between the Total Overlap S^ρ (in $e^2\,a_0^{-3}$) and the Exchange−Repulsion Energy E_{rep} (in E_h)[a] Evaluated Using IMPT at the Orientations Shown in Figure 2

basis set for IMPT	basis set for overlaps	K/a.u.	r^2 of fit
	Total overlaps		
6-31G**	6-31G**	7.241289	0.99267
6-31G**	6-311G**	6.895594	0.99730
6-31G**	cc-pVDZ	7.371801	0.99708
6-31G**	aug-cc-pVDZ	5.658931	0.97121
	Model Overlaps		
6-31G**	6-31G**	5.76951	0.98419
6-31G**	6-311G**	6.21180	0.98614
6-31G**	cc-pVDZ	4.19921	0.98214
6-31G**	aug-cc-pVDZ	4.83504	0.29744
cc-pVDZ	cc-pVDZ	4.155294	0.97782

[a] $E_h = 2.6255 \times 10^3$ kJ/mol.

When the pre-exponential factor was fitted to the sets of total atom−atom overlaps, the changes from the $A_{\iota\kappa}$ values derived from the analytic isotropic coefficient C_{000}^{00} using the same $\alpha_{\iota\kappa}$ (contrast $A_{\iota\kappa} = Ks_{\iota\kappa}^{\text{anal}}$ and $A_{\iota\kappa} = Ks_{\iota\kappa}^{\text{fit}}$ in Table 2) varied from an insignificant few percent to being quite substantial. The most significant change for the atom types, which were well sampled by the crystal structures and by the fitting, was a 20% decrease for the $H\cdots O_1$ for both the 6-31G** and cc-pVDZ overlaps. The 6-311G** model gave an unphysically large H···H parameter on fitting and so this parameters set was not considered further. The quality of fits for the 6-31G** model did not change significantly when the $\alpha_{\iota\kappa}^{\text{formic}}$ parameters derived from the large basis set calculations on formic acid were used, instead of those derived from this basis set, though the $s_{\iota\kappa}$ values did change to compensate for the $\alpha_{\iota\kappa}$ changes, giving the potential parameters in Table 3.

3.2 Testing on the Oxalic Acid Crystal Structures. The test of the various repulsion models is provided by their ability to reproduce the crystal structures of the two polymorphs of oxalic acid. The differences between the relaxed crystal structures and the room-temperature experimental starting point for many of the model potentials investigated is given in Table 4.

The first set of entries shows the structures corresponding to the various DMA electrostatic models, used in conjunction with

TABLE 2: Model Repulsion Potential Parameters Derived from the Overlap of Various Ab Initio Charge Densities of Oxalic Acid

Charge density	MP2 631G**			MP2 6-311G**			MP2 cc-pVDZ			MP2 aug-cc-pDVZ	
Atom types	$\alpha_{\iota\kappa}$ (Å^{-1})	$A_{\iota\kappa} = Ks_{\iota\kappa}^{anal}$ (kJ mol^{-1})	$A_{\iota\kappa} = Ks_{\iota\kappa}^{fit}$ (kJ mol^{-1})	$\alpha_{\iota\kappa}$ (Å^{-1})	$A_{\iota\kappa} = Ks_{\iota\kappa}^{anal}$ (kJ mol^{-1})	$A_{\iota\kappa} = Ks_{\iota\kappa}^{fit}$ (kJ mol^{-1})	$\alpha_{\iota\kappa}$ (Å^{-1})	$A_{\iota\kappa} = Ks_{\iota\kappa}^{anal}$ (kJ mol^{-1})	$A_{\iota\kappa} = Ks_{\iota\kappa}^{fit}$ (kJ mol^{-1})	$\alpha_{\iota\kappa}$ (Å^{-1})	$A_{\iota\kappa} = Ks_{\iota\kappa}^{anal}$ (kJ mol^{-1})
C···C	4.48	778879	730111	4.12	368366	500775	4.01	346951	330821	2.29	18371
C···O_1	4.62	1720687	1841792	4.37	1049243	1258419	4.26	729734	616070	2.88	63158
C···O_2	4.63	1560983	1326880	4.39	911792	959936	4.32	702776	521332	2.67	37913
O_1···O_1	4.74	3638547	3635198	4.59	2761141	2928355	4.72	2344708	2548566	9.56	44268251241
O_1···O_2	4.80	3818015	3697650	4.74	3400993	2967239	4.90	2775570	2466202	8.02	2046997716
O_2···O_2	4.85	3896834	3784513	4.91	4248155	3456582	5.03	2705049	2548721	6.80	241081343
H···C	4.26	39790	25166	3.51	5233	5819	3.81	17140	11750	3.25	8952
H···O_1	4.12	51707	41075	4.33	73796	75640	4.17	46686	36908	6.24	893095
H···O_2	4.22	57636	51971	4.59	103926	137355	4.43	63197	66893	6.68	1543831
H···H	4.27	4349	3722	5.54	28617	99426	4.47	6493	6517	7.31	364478

TABLE 3: Set of Isotropic Atom−Atom Repulsion−Dispersion Parameters for Oxalic Acid

	$\alpha_{\iota\kappa}^{formic\ a}$ (Å^{-1})	$A_{\iota\kappa}$ (kJ mol^{-1})	$C_{\iota\kappa}{}^{b}$ (kJ mol^{-1} Å^6)
C···C	4.19	281709	1359.7
C···O_1	3.93	222343	1383.0
C···O_2	4.23	400397	1045.3
O_1···O_1	3.72	179954	1429.5
O_1···O_2	3.87	291426	1092.5
O_2··O_2	4.15	531780	841.5
H···C	4.27	25828	523.9
H···O_1	3.91	28181	523.2
H···O_2	4.04	38118	390.6
H···H	4.19	3186	206.3

[a] The repulsion parameters are those derived using the $\alpha_{\iota\kappa}^{formic}$ parameters from a large basis set calculation on formic acid and fitting $s_{\iota\kappa}$ to the oxalic acid dimer overlaps calculated using a MP2/6-31G** charge density. [b] The dispersion coefficients $C_{\iota\kappa}$ are derived from the Slater−Kirkwood model.

a transferable empirical repulsion−dispersion potential. The empirical model potential used was based on Williams potentials for C and O,[5] with the polar hydrogen parameters initially derived for N−H hydrogen bond donors (FIT[10]) being scaled to reproduce the crystal structures of a range of carboxylic acids.[16] Hence, it is not surprising that these potentials represent the hydrogen bond lengths (and hence *a* parameter of the β form) extremely well, and indeed the α polymorph is represented very well for a static lattice energy minimization. However, the *b* and *c* parameters of the β form have unacceptable errors of over ±10%, corresponding to a change in the relative tilt of the dimer chains in their herringbone motif. These structural changes correspond to an energy lowering of less than 3.5 kJ/mol. Varying the basis set used to calculate the electrostatic interactions has a minor effect on the calculated crystal structures, relative to the few percent error which may be attributable to comparing lattice energy minima with room-temperature structures. However, it does affect the lattice energies somewhat, as the electrostatic contribution to the total lattice energy at the experimental structures is 84% for the α form and 94% for the β form.

In contrast to the above and published model potentials, which have been empirically fitted to crystal structure and sublimation data, the potentials constructed in this work, without reference to any crystal structures, perform remarkably well (Table 4). All of the models constructed give a plausible representation of both polymorphs, though there are still errors which vary with the method and charge distribution used to construct the repulsion model. The cc-pVDZ model does less well than the more standard 6-31G** and 6-311G** basis sets throughout, with a tendency for a significant contraction along the *c* direction in the β form, giving a shorter stacking distance of the carboxylic dimer chains. The basic overlap model, derived from the analytical isotropic coefficient, gives a good account of the relative tilt of the dimeric chains in the β polymorph, but overestimates the hydrogen bond lengths, and hence has a poor *a* parameter for the β form and *b* parameter for the α polymorph. This elongation of the hydrogen bond lengths is somewhat remedied by the fitting of the pre-exponential factor directly to the atom−atom overlaps, which reduces the H···O_1 repulsion. The use of the formic acid exponents gives a comparable structure prediction, which is reasonably satisfactory for both polymorphs, within the limitations of comparing static lattice energy minima with room-temperature structures.

3.3 Evaluation of Calculated Lattice Energies. The model potentials can also be assessed on the accuracy of the predicted lattice energies, by comparing these to the experimental heats of sublimation, although there is some uncertainty in the experimental values. The study of Bradley and Cotson[52] determined the experimental sublimation energies to be 97.9 kJ/mol for the α and 93.3 kJ/mol for the β polymorph, in good agreement with the results of de Wit et al.[53] (98.5 and 92.5 kJ/mol for the α and β polymorphs, respectively), but higher than the 93.7 ± 0.8 kJ/mol reported for the α form from vapor pressure measurements.[13] The α-to-β heat of transition was found to be 1.3 ± 0.2 kJ/mol by differential scanning calorimetry.[13] However, a more recent study by Stephenson and Malanowski[54] estimates a difference of only 0.1 kJ/mol between the sublimation energies of the two polymorphs, with a sublimation enthalpy of 93.4 kJ/mol for the α and 93.3 kJ/mol for the β form.

The comparison of calculated lattice energies with heats of sublimation involves various approximations, leading to general estimates of between 8 [55] to 15 [3] kJ/mol of the significance threshold for the comparison. In the case of carboxylic acids, the contribution of the internal energy difference between the molecule in each crystal structure and the gas phase is particularly difficult to estimate, as there is the possibility that the apparent carboxylic acid group geometry in the crystal is distorted by disorder in the proton position. The intramolecular geometry of oxalic acid differs significantly between the two crystal structures,[35] with the carboxylic acid in the α form bearing a closer resemblance to the experimental electron density gas-phase structure[56] than the molecule in the β structure. The C═O_1 bond is longer and C−O_2 is shorter, both by 0.016 Å in the β polymorph. This means that in the β form the difference between the C−O_2 and C═O_1 bond lengths is 0.063 Å, only slightly greater than the 0.05 Å limit[9] used to remove crystal structures likely to be affected by proton disorder from an analysis of carboxylic group hydrogen bond geometries. In both polymorphs, the molecule is basically planar, but the hydrogen

TABLE 4: Errors in the Reproduction of the Crystal Structures of α- and *β*-Oxalic Acid, with Various Atom−Atom Model Intermolecular Potentials

potential			errors in reproduction of crystal structures[a]										lattice energy kJ mol^{-1}	
			α form OXALAC03					*β* form OXALAC04						
basis set	repulsion	dispersion	Δ*a*/Å	Δ*b*/Å	Δ*c*/Å	Δ*V*/%	RMS/%	Δ(O···O)/Å	Δ*a*/Å	Δ*b*/Å	Δ*c*/Å	Δ*β*/°	Δ*V*/%	RMS/%	Δ(O···O)/Å	α	*β*
Empirical Repulsion−Dispersion + DMA Electrostatic																	
6-31G**	FITOH	FIT	0.161	0.065	−0.050	2.5	1.6	−0.008	−0.021	0.677	−0.878	−3.5	−4.5	11.4	−0.010	−101.3	−114.9
6-311G**	FITOH	FIT	0.147	−0.103	0.073	2.1	1.7	−0.009	−0.046	0.781	−0.939	−3.5	−4.8	12.4	−0.042	−100.2	−116.5
cc-pVDZ	FITOH	FIT	0.158	−0.102	0.136	3.3	2.0	0.014	−0.014	0.766	−0.904	−3.3	−3.8	12.1	−0.007	−94.1	−108.9
Overlap Repulsion Derived Analytically from C_{000}^{00}, Slater−Kirkwood Dispersion + DMA Electrostatic																	
6-31G**	$Ks_{ik}^{anal}\alpha_{ik}$	S−K	−0.122	0.709	−0.171	4.0	5.6	0.285	0.314	−0.044	−0.153	3.58	−1.1	3.8	0.338	−101.4	−104.8
6-311G**	$Ks_{ik}^{anal}\alpha_{ik}$	S−K	0.013	0.626	−0.129	5.9	4.8	0.288	0.312	0.137	−0.226	3.85	0.2	4.3	0.332	−97.9	−102.8
cc-pVDZ	$Ks_{ik}^{anal}\alpha_{ik}$	S−K	−0.141	0.511	−0.314	−1.2	5.0	0.176	0.191	0.233	−0.817	0.56	−9.0	9.2	0.221	−104.7	−115.5
Overlap Repulsion Derived by Fitting to Atom−Atom Overlaps, Slater−Kirkwood Dispersion + DMA Electrostatic																	
6-31G**	$Ks_{ik}^{fit}\alpha_{ik}$	S−K	−0.085	0.385	−0.073	2.3	3.0	0.198	0.198	−0.037	−0.185	2.8	−2.9	2.5	0.213	−106.1	−113.1
cc-pVDZ	$Ks_{ik}^{fit}\alpha_{ik}$	S−K	−0.233	−0.174	−0.068	−6.8	2.5	0.049	0.029	0.001	−0.784	−1.9	−12.6	8.3	0.041	−116.7	−131.9
Overlap Repulsion Derived by Fitting to Atom−Atom Overlaps Using Formic Acid α Values, Slater−Kirkwood Dispersion + DMA Electrostatic																	
6-31G**	$Ks_{ik}^{fit}\alpha_{ik}^{formic}$	S−K	−0.174	0.438	−0.112	0.9	3.7	0.185	0.168	−0.089	−0.19	1.92	−3.6	2.8	0.179	−100.0	−105.8
Using Ab Initio Optimized Molecular Structure																	
6-31G**	$Ks_{ik}^{fit}\alpha_{ik}^{formic}$	S−K	−0.165	0.555	−0.125	2.2	4.5	0.187	0.226	−0.037	−0.315	0.04	−2.4	4.2	0.227	−92.9	−93.8

[a] The errors are defined Δ = minimized − experimental. The RMS % error is taken over the three cell lengths.

atom is out of the plane of the molecule, with the torsion angle O_1-C-O_2-H being 4.6° for the α and 4.4° for the *β* polymorph. Thus, the differences between the molecular structures in the two polymorphs are affected by the errors in the crystal structure determination due to static proton disorder, which is probably greater in the carboxylic acid dimer motif of the *β* form, as well as the usual effects of different packing environments.

All basis sets predict the geometry of the α form (OXALAC03) to be more stable than that of the *β* (OXALAC04) by about 8 kJ/mol at the MP2 level (varying from 7.6 kJ/mol for aug-cc-pVDZ to 9.45 for 6-311G**). All calculations predict that the α form is about 18 ± 1 kJ/mol less stable than the gas-phase geometry obtained by optimization at the MP2 level using a 6-31G** basis set. There is a significant difference between the optimized O−H bond length of 0.971 Å and the 1.02 Å assumed for the bond length in the crystal from the average neutron value,[38] (which itself may be slightly affected by disorder, although structures where this was explicitly reported were removed). There is also a small lengthening of the $C-O_1$ bond length. It is therefore uncertain how much of the calculated differences in internal energy is genuine and how much is artifacts of the errors in the theoretical or experimental methods (the *R* factors are 0.053 for α and 0.073 for *β* forms). Although the intramolecular energy difference between the molecular geometry in the two crystal phases is reasonably small, it will contribute to the difference in the experimental heats of sublimation of the two polymorphs, which are assumed measured relative to the most stable gas phase conformer.

Given the above uncertainties, the lattice energies predicted by the various model potentials (Table 4) are all quite reasonable. The *β* polymorph has a more negative lattice energy than the α form in all calculations, with the difference being between 3 and 7 kJ/mol for the potentials that reproduce both structures. Given that this is just less than the estimated difference in the intramolecular structures (8 kJ/mol) favoring the α form, the calculations are correctly predicting that there is very little difference in the energies for the two forms. To confirm the effects of the uncertainty in the molecular structure, the ab initio optimized molecular structure was also used with the corresponding DMA and α^{formic} based repulsion−dispersion potential to model both polymorphs. The final entry in Table 4 shows that this gives a slightly worse but acceptable reproduction of the crystal structures. It significantly reduces both lattice energies, the *β* form more than the α form, to values comparable with experimental ΔH_{sub} values,[54] so that the *β* form is more stable than the α form by less than 1 kJ mol^{-1}. The fact that all of the lattice energies are plausible, given that the model potentials were all constructed without reference to any total energy estimates, let alone experimental heats of sublimation, is most encouraging. However, improvements to the dispersion energy model are likely to have a more significant effect on the lattice energy than the structure, and there is some basis set dependence to the dominant electrostatic energy contribution, so there may be some fortuitous cancellation of errors.

4. Discussion and Conclusions

This method of constructing a model potential from the properties of the isolated molecule is remarkably successful at predicting the solid state properties of oxalic acid, particularly in comparison with using empirical carboxylic acid potentials to extrapolate from experimental data. The results are still sensitive to the approximations made in the derivation of the

repulsion potential from the overlap of the charge distribution, and this study has shown some of the strengths and pitfalls of this approach. There are other approximations in the model potential, including a rather crude dispersion model. However, this study confirms that the basic approach is practical and reasonably accurate. It is an approach that can be readily applied to organic molecules where the available transferable potentials are not adequate or the study warrants a specifically derived model potential. We are currently investigating the application of this approach to groups of organic molecules, to establish what factors govern when it is worth deriving a specific potential.

The study has revealed that the application of the overlap model is quite sensitive to the basis set applied, and that the usual energetic criterion for quality of basis sets does not apply. The overlap will be most readily represented by an exponential atom−atom model when the basis set provides an exponentially decaying tail to the wave function. The division of the overlap/repulsion into atom−atom contributions, which is a great advantage of the overlap model, will be basis set dependent. Both of these aspects may become unstable/unphysical when a basis set contains a limited number of diffuse functions, and so the wave function does not decay exponentially with distance. Fortunately, such problems become apparent in the analysis, as our results for aug-cc-pVDZ basis set show. The correlation of the α and s parameters, and their dependence on the exponential tail of the wave function, does suggest that it may be better to extract the α parameters from an accurately exponentially decaying wave function (large basis set), if necessary, for a smaller model molecule. The significant correlation between the pre-exponential ($A_{t\kappa}$) and slope ($\alpha_{t\kappa}$) parameters in model repulsion potentials suggests that any errors in assuming transferability of the $\alpha_{t\kappa}$ parameters may be compensated for quite well by the fitting of the $A_{t\kappa}$ parameters for the specific molecule.

A further approximation to the repulsion potential that was made in this work was to assume that each atom−atom repulsion was isotropic. We have confirmed the previous observation[24] that the isotropic term in the analytical expansion of the overlap is not necessarily the most effective isotropic term for the intermolecular region. This is because the analytical expansion for the atom−atom overlap converges very slowly, as it is representing the atomic charge distribution in the bonding as well as the nonbonding region around each nucleus. Thus fitting the coefficient to the atom−atom overlaps in the region of the intermolecular potential would be expected to give a better representation of the intermolecular overlaps and hence repulsion. It would allow an effective anisotropic repulsion model to be derived, or the error in assuming that the repulsion was isotropic to be assessed, if the fitting was done to a larger set of atom−atom overlaps chosen to represent all of the intermolecular repulsive region around each atom.

A key stage in the use of the overlap model is the determination of the proportionality constant between the total model for the molecule−molecule overlap and the repulsion. We had originally intended that the fitting to a small number of ab initio IMPT exchange−repulsion energies would provide just a first estimate of K, as well as some cross checking on the model. However, the results suggested that it was not worth refining the value of K against the experimental data, given the errors intrinsic in the comparison. However, this one empirical factor could be fitted in other applications, and indeed this might be preferable, as it would have the advantage of absorbing the error due to the neglect of other exponentially decaying terms,

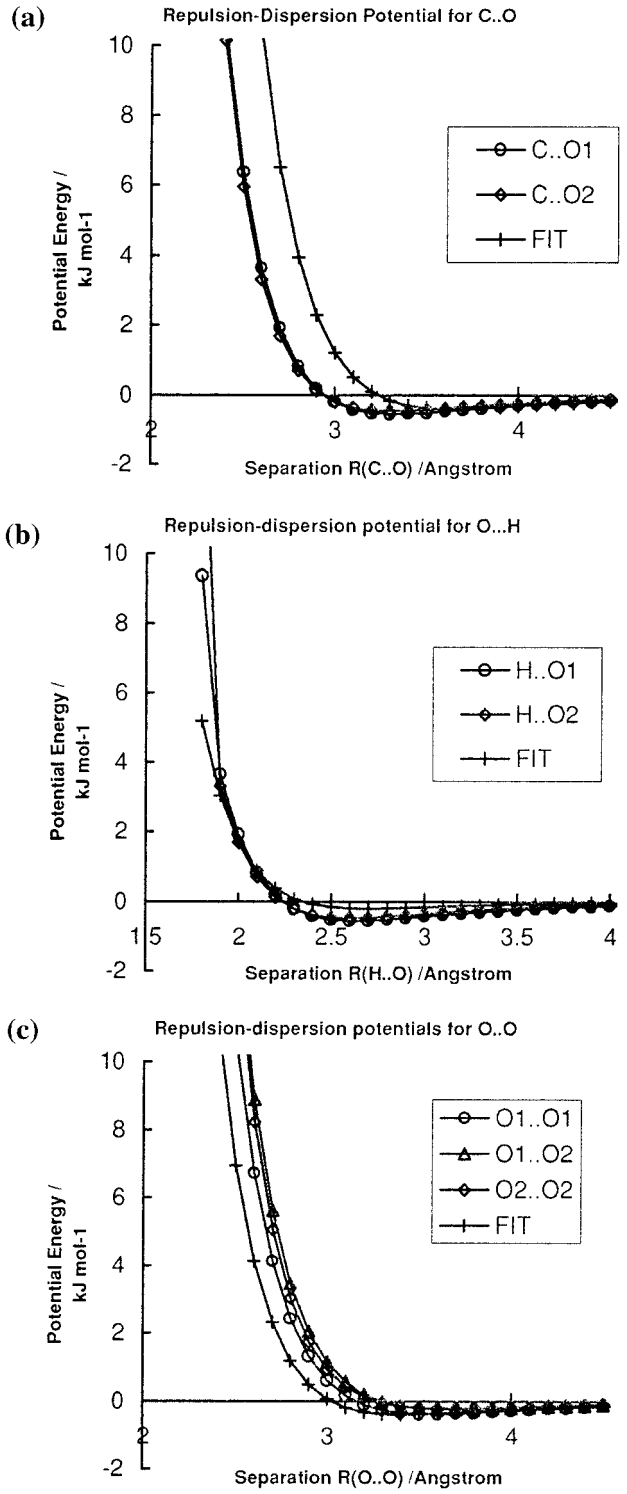

Figure 3. Comparison of the atom−atom repulsion−dispersion potentials for (a) C···O, (b) O···H, and (c) O···O. The potentials for O_1 and O_2 are those developed in this paper, using $\alpha_{t\kappa}^{\text{formic}}$ and $A_{t\kappa}^{\text{fit}}$ and C parameters as given in Table 3. The FIT potential parameters are empirically fitted to crystal structure data, the parameters for C and O were fitted to oxyhydrocarbons,[5] with the parameter set extended to O···H for carboxylic acids.[16]

such as the effect of the overlap on the long-range terms (electrostatic penetration, dispersion damping etc.) and any charge transfer.

The dispersion model could be improved when atom−atom dispersion coefficients can be reliably calculated from the charge densities of the isolated molecules. Considerable progress is

being made in this direction.[57] The Slater−Kirkwood based model omits the anisotropy or higher terms in the atom−atom dispersion and the damping effects. The use of experimentally tabulated atomic polarizabilities[51] results in a marked difference between the two types of oxygen atoms and a rather large dispersion coefficient associated with the hydrogen atom.

Despite these limitations, the model potentials do give quite reasonable reproduction of the two polymorphs of oxalic acid, such that the remaining errors may be mainly due to other assumptions in the simulation. The overlap model parameters are somewhat overestimating the hydrogen bond lengths, which are not atypical of carboxylic acid structures.[9] Changing the assumed O_1-H bond length from the average neutron value of 1.02 Å to the ab initio gas-phase optimized value of 0.971 Å only makes a small difference to the hydrogen bond lengths in the β form and none to the α form, so it is probable that the polar hydrogen potential could still be improved, possibly by incorporating repulsion anisotropy. The difference in $C=O_2$ and $C-O_1$ bond lengths between the two crystal structures will have contributed to the estimated difference in internal energies, so the possibility of disorder adds to the usual problems in comparing the various experimental values for the heat of sublimation with the lattice energy. This is in addition to the usual problems in comparing lattice energy minima (effectively 0 K) with experimental room-temperature structures for organic systems, where the structure suggests that thermal expansion effects will be very anisotropic. Thus, we expect that future testing of the overlap model predictions against spectroscopic data for organic systems may be more revealing of the strengths and problems of this method of deriving repulsion potentials.

In the specific case of oxalic acid, the model potential developed in this work differs crucially from the empirically transferable potentials in that it does not assume that the repulsion−dispersion is the same for the hydroxyl and carbonyl oxygens or that the carbon atom is the same as that in other organic compounds. (Indeed, the carbon atom in oxalic acid differs from that in all other carboxylic acids in that it is unable to gain electron density from the rest of the molecule.) Nevertheless, it is encouraging that the model potentials derived in this paper are physically reasonable and not too dissimilar from the empirical potentials, as shown in Figure 3. The model repulsion−dispersion potential of Table 3 is very similar for O_1 and O_2 interacting with either the hydrogen or the carbon atom (Figures 3a and 3c), though the differences are more marked for the O···O interactions. The similarity of the potential curves shows that there is considerable compensation between the rather different A and α parameters for the O_1 and O_2 interactions (Table 3). The well depths for interaction with O_1 are slightly deeper than those for O_2, as there is a slightly greater dispersion coefficient for the more polarizable carbonyl oxygen. The differences between the potentials derived in this paper and the empirical potential for carboxylic acids (Figure 3) are plausible. The O···H and O···O potentials are similar, with the empirical potentials being less repulsive at the crystallographic hydrogen bonding separations that they were optimized to reproduce. This is consistent with the overestimate of the hydrogen bond lengths in the crystal by the gas phase derived potentials. Our specific potential for oxalic acid is significantly less repulsive than the empirical potential for the close $C\cdots O_2$ distances of 2.90 and 3.02 Å sampled in the β form, consistent with the ability of the specific potential to reproduce the β form structure better than the empirical potential. The fact that this repulsion−dispersion model does predict the structure of β-oxalic acid reasonably well, in contrast to the empirical models, is consistent with the conclusion[58] that the offset between the glide-related hydrogen bonded chains is determined primarily by the van der Waals rather than the electrostatic forces. Another advantage of the overlap model is that no combining rules need be assumed for the repulsion parameters. The overlap derived repulsion parameters are in poor agreement with the usual combining rules $\alpha_{\iota\kappa} = (\alpha_{\iota\iota} + \alpha_{\kappa\kappa})/2$ and $A_{\iota\kappa} = (A_{\iota\iota}A_{\kappa\kappa})^{1/2}$.

This study has derived an intermolecular potential for oxalic acid from the properties of the isolated molecule, concentrating on the derivation of the repulsion potential parameters from the ab initio calculated overlap of the charge distributions. The resulting potential gives a better account of the two polymorphic structures of oxalic acid than traditional empirical potentials, particularly with regard to the relative tilt of the hydrogen bonded chains in the β polymorph. Thus, the methodology seems very promising for developing model potentials for organic molecules with fewer assumptions.

Acknowledgment. We thank Dr R. J. Wheatley for the use of the GMUL program and useful discussions, Theresa Beyer for some data, the Cambridge Crystallographic Database for providing a research studentship for I.N., and the EPSRC for support.

References and Notes

(1) Wiberg, K. B.; Rablen, P. R. *J. Comput. Chem.* **1993**, *14*, 1504.
(2) Price, S. L. *J. Chem. Soc., Faraday Trans.* **1996**, *92*, 2997.
(3) Pertsin, A. J.; Kitaigorodsky, A. I. *The Atom-Atom Potential Method. Applications to Organic Molecular Solids*; Springer-Verlag: Berlin, 1987; Vol. 43.
(4) Williams, D. E.; Cox, S. R. *Acta Crystallogr. B* **1984**, *40*, 404.
(5) Cox, S. R.; Hsu, L. Y.; Williams, D. E. *Acta Crystallogr. A* **1981**, *37*, 293.
(6) Hagler, A. T.; Huler, E.; Lifson, S. *J. Am. Chem. Soc.* **1974**, *96*, 5319.
(7) Lifson, S.; Hagler, A. T.; Dauber, P. *J. Am. Chem. Soc.* **1979**, *101*, 5111.
(8) Filippini, G.; Gavezzotti, A. *Acta Crystallogr. B* **1993**, *49*, 868.
(9) Gavezzotti, A.; Filippini, G. *J. Phys. Chem.* **1994**, *98*, 4831.
(10) Coombes, D. S.; Price, S. L.; Willock, D. J.; Leslie, M. *J. Phys. Chem.* **1996**, *100*, 7352.
(11) Price, S. L.; Stone, A. J. *Mol. Phys.* **1984**, *51*, 569.
(12) Hagler, A. T.; Dauber, P.; Lifson, S. *J. Am. Chem. Soc.* **1979**, *101*, 5131.
(13) Derissen, J. L.; Smit, P. H. *Acta Crystallogr. A* **1978**, *34*, 842.
(14) Smit, P. H.; Derissen, J. L.; van Duijneveldt, F. B. *Mol. Phys.* **1979**, *37*, 521.
(15) Leiserowitz, L. *Acta Crystallogr. B* **1976**, *32*, 775.
(16) Beyer, T.; Price, S. L., in preparation.
(17) Scheiner, S. *Reviews in Computational Chemistry*; Lipkowitz, K. B., Boyd, D. B., Eds.; VCH: New York, 1991; Vol. 2, p 165.
(18) Stone, A. J. *The Theory of Intermolecular Forces*, 1st ed.; Clarendon Press: Oxford, 1996; Vol. 32.
(19) Price, S. L. *Philos. Mag.* **1996**, *73*, 95.
(20) Price, S. L. *Reviews in Computational Chemistry*; Lipkowitz, K. B., Boyd, D. B., Eds.; Wiley: New York, 1999.
(21) Wheatley, R. J.; Price, S. L. *Mol. Phys.* **1990**, *69*, 507.
(22) Kim, Y. S.; Kim, S. K.; Lee, W. D. *Chem. Phys. Lett.* **1981**, *80*, 574.
(23) Kita, S.; Noda, K.; Inouye, H. *J. Chem. Phys.* **1976**, *64*, 3446.
(24) Nobeli, I.; Price, S. L.; Wheatley, R. J. *Mol. Phys.* **1998**, *95*, 525.
(25) Beu, T. A.; Buck, U.; Ettischer, I.; Hobein, M.; Siebers, J.-G.; Wheatley, R. J. *J. Chem. Phys.* **1997**, *106*, 6806.
(26) Beu, T. A.; Buck, U.; Siebers, J.-G.; Wheatley, R. J. *J. Chem. Phys.* **1997**, *106*, 6795.
(27) Buck, U.; Siebers, J.-G.; Wheatley, R. J. *J. Chem. Phys.* **1998**, *108*, 20.
(28) Wheatley, R. J.; Hutson, J. M. *Mol. Phys.* **1995**, *84*, 879.
(29) Wheatley, R. J. *Mol. Phys.* **1996**, *87*, 1083.
(30) Wallqvist, A.; Ahlstrom, P.; Karlstrom, G. *J. Phys. Chem.* **1990**, *94*, 1649.
(31) Stone, A. J.; Tong, C. S. *J. Comput. Chem.* **1994**, *15*, 1377.
(32) Wheatley, R. J.; Mitchell, J. B. O. *J. Comput. Chem.* **1994**, *15*, 1187.

(33) Stone, A. J. *Chem. Phys. Lett.* **1981**, *83*, 233.
(34) Slater, J. C.; Kirkwood, J. G. *Phys. Rev.* **1931**, *37*, 682.
(35) Derissen, J. L.; Smit, P. H. *Acta Crystallogr. B* **1974**, *30*, 2240.
(36) McKinnon, J. J.; Mitchell, A. S.; Spackman, M. A. *Chemistry−Eur. J.* **1998**, *4*, 2136.
(37) Allen, F. H.; Kennard, O. *Chem. Design Automation News* **1993**, *8*, 1, 31.
(38) Allen, F. H.; Kennard, O.; Watson, D. G.; Brammer, L.; Orpen, A. G.; Taylor, R. *J. Chem. Soc., Perkins Trans. 2* **1987**, S 1.
(39) Willock, D. J.; Price, S. L.; Leslie, M.; Catlow, C. R. A. *J. Comput. Chem.* **1995**, *16*, 628.
(40) Amos, R. D. with contributions from Alberts, I. L.; Andrews, J. S.; Colwell, S. M.; Handy, N. C.; Jayatilaka, D.; Knowles, P. J.; Kobayashi, R.; Koga, N.; Laidig, K. E.; Laming, G.; Lee, A.; Maslen, P. E.; Murray, C. W.; Rice, J. E.; Simandiras, E. D.; Stone, A. J.; Su, M. D.; Tozer, D. J. *CADPAC6: The Cambridge Analytical Derivatives Package*; 6.0 ed.: Cambridge, 1995.
(41) Hehre, W. J.; Ditchfield, R.; Pople, J. A. *J. Chem. Phys.* **1972**, *56*, 2257.
(42) Krishnan, R.; Binkley, J. S.; Seeger, R.; Pople, J. A. *J. Chem. Phys.* **1980**, *72*, 650.
(43) Dunning, T. H. *J. Chem. Phys.* **1989**, *90*, 1007.
(44) Wheatley, R. J. GMUL 3s. An extension to the GMUL program (version 3) that calculates an analytical form for the overlap of distributed charge densities.; University of Nottingham, 1997.
(45) Stone, A. J. *Mol. Phys.* **1979**, *36*, 241.
(46) *Microsoft EXCEL*; 5.0a ed., Microsoft Corporation 1985−1993.
(47) Hayes, I. C.; Stone, A. J. *Mol. Phys.* **1984**, *53*, 83.
(48) Hayes, I. C.; Hurst, G. J. B.; Stone, A. J. *Mol. Phys.* **1984**, *53*, 107.
(49) Stone, A. J. *Chem. Phys. Lett.* **1993**, *211*, 101.
(50) Pitzer, K. S. *Adv. Chem. Phys.* **1959**, *11*, 59.
(51) Ketelaar, J. A. A. *Chemical Constitution*; Elsevier: Amsterdam, 1953.
(52) Bradley, R. S.; Cotson, S. *J. Chem. Soc.* **1953**, 1684.
(53) de Wit, H. G. M.; Bouwstra, J. G.; Blok, J. G.; de Kruif, C. G. *J. Chem. Phys.* **1983**, *78*, 1470.
(54) Stephenson, R. M.; Malanowski, S. *Handbook of Thermodynamics of Organic Compounds*; Elsevier: New York, 1987.
(55) Gavezzotti, A. *Theoretical Aspects and Computer Modeling of the Molecular Solid State*; Gavezzotti, A., Ed.; John Wiley & Sons: Chichester, 1997; Vol. 1, p 97.
(56) Nahlovska, Z.; Nahlovshy, B.; Strand, T. G. *Acta Chem. Scand.* **1970**, *24*, 2617.
(57) Amos, R. D.; Ioannou, A. G., in preparation.
(58) Berkovitch-Yellin, Z.; Leiserowitz, L. *J. Am. Chem. Soc.* **1982**, *104*, 4052.
(59) Etter, M. C. *Acc. Chem. Res.* **1990**, *23*, 120.
(60) Stone, A.; Dullweber, A.; Hodges, M. P.; Popelier, P. L. A.; Wales, D. J. *ORIENT*, 3.2 ed.; University of Cambridge, 1996.